ELECTRONIC SUPPORTING INFORMATION FOR

Integration of the evaporable spin crossover complex [Fe(HB(1,2,4-triazol-1-yl)3)2] into organic field effect transistors: towards multifunctional OFET devices

Yuteng Zhang, Isabelle Séguy, Ion Soroceanu, Aurelian Rotaru, Haizhu Yu, Lionel Salmon, Gábor Molnár, Azzedine Bousseksou**

Yuteng Zhang, Lionel Salmon, Gábor Molnár, Azzedine Bousseksou
LCC, CNRS and Université de Toulouse, UPS, INP, F-31077 Toulouse, France
E-mail: gabor.molnar@lcc-toulouse.fr, azzedine.bousseksou@lcc-toulouse.fr

Yuteng Zhang, Isabelle Séguy
LAAS, CNRS and Université de Toulouse, INSA, UPS, F-31077 Toulouse, France

Ion Soroceanu, Aurelian Rotaru
Faculty of Electrical Engineering and Computer Science and MANSiD Research Center, Stefan cel Mare University, 13, Strada Universitatii, Suceava 720229, Romania

Haizhu Yu
Department of Chemistry and Centre for Atomic Engineering of Advanced Materials, Key Laboratory of Structure and Functional Regulation of Hybrid Materials of Ministry of Education, Institutes of Physical Science and Information Technology and Anhui Province Key, Laboratory of Chemistry for Inorganic/Organic Hybrid Functionalized Materials, Anhui University, Hefei, China

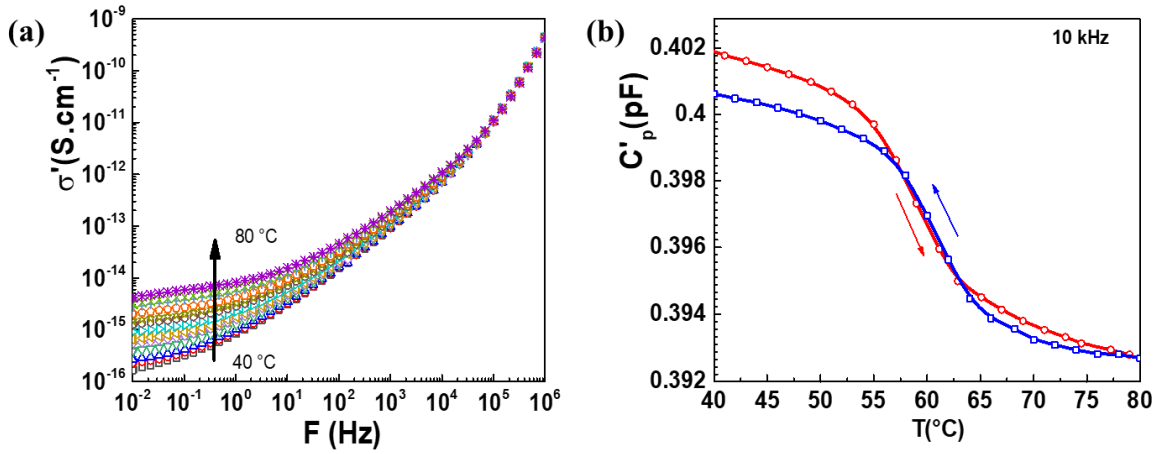

Figure S1: (a) Variable temperature conductivity spectra and (b) capacitance (10 kHz) of a ITO/[Fe(HB(tz)$_3$)$_2$]/Al junction extracted from impedance measurements.

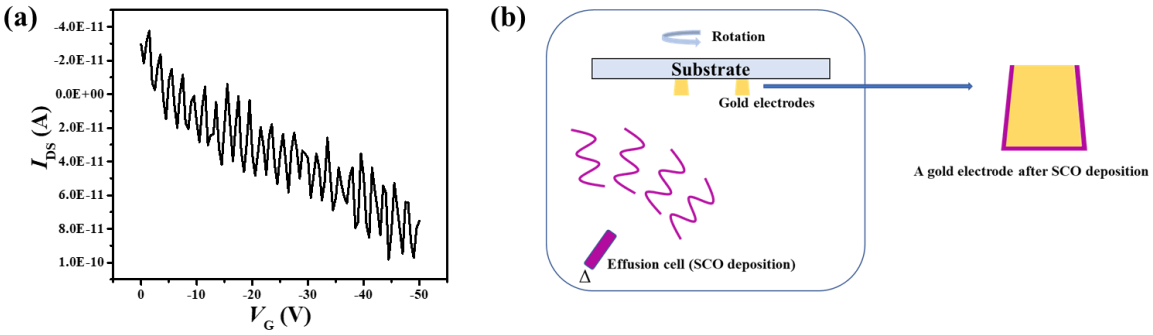

Figure S2: (a) Representative transfer characteristic (V_{DS} = -30 V) of Device A, channel width W = 50 µm, channel length L = 1500 µm. (b) The scheme of SCO deposition on the 'wall' of Au electrodes.

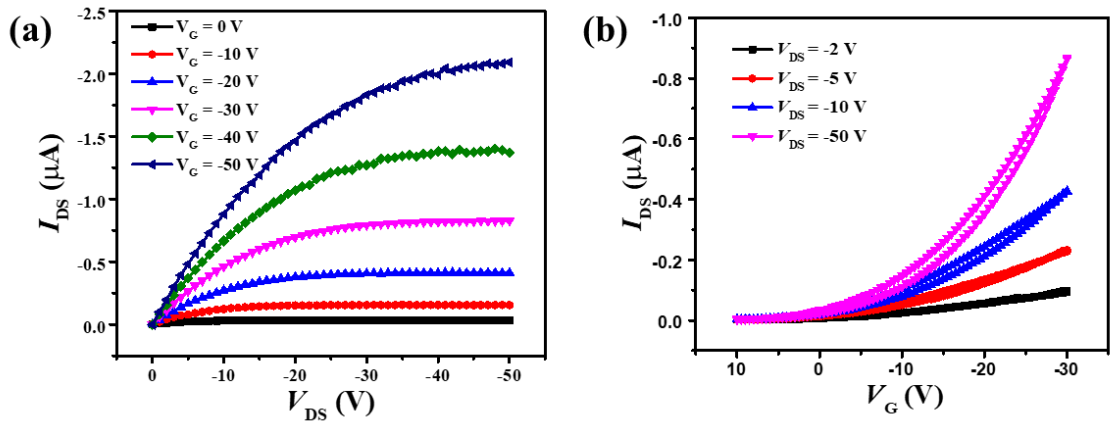

Figure S3: (a) Output (V_G = 0, -10, -20, -30, -40 and -50 V) and (b) transfer characteristic (V_{DS} = -2, -5, -10 and -50 V) of a 'blank device' (same as Device B, but without SCO) measured at 45 °C. W = 70 µm, L = 1000 µm.

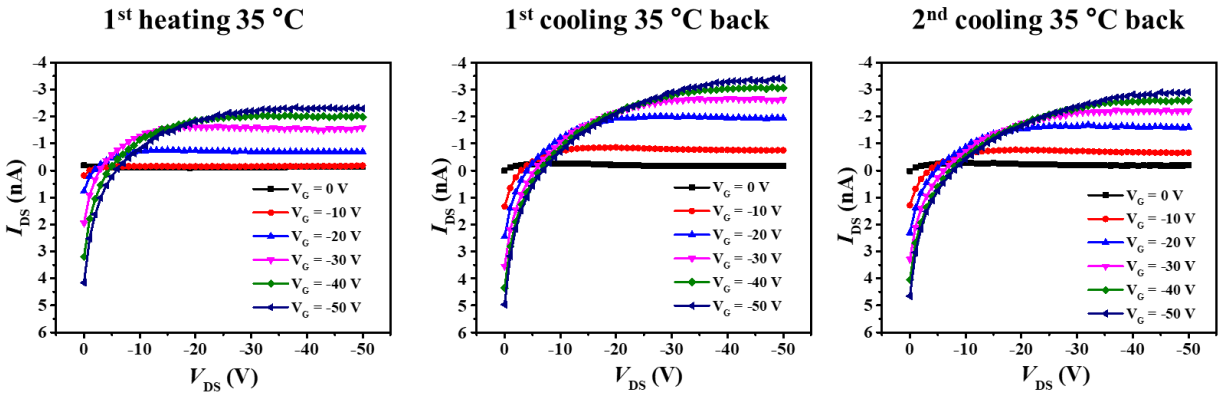

Figure S4: Output characteristics of Device B before/after thermal cycles between 35 and 70 °C. W = 50 µm, L = 1000 µm.

Development of the transistor characterization protocol

To establish a reliable protocol to characterize the OFETs at elevated temperatures, a series of experiments had been conducted to minimize the impact from temperatures. The transistor we investigated here has a bottom gate/top contact configuration, with 50 nm thickness of benzo[a]hexacene as OSC layer (without SCO layer). For convenience, we will cite this transistor as the 'standard device'. Because our key interest is the temperature-dependent characteristics of the transistor, experiments were carried out in many thermal cycles with different conditions. Table S1 shows the main parameters for six successive thermal cycles on a standard device. The temperature range is the same in the first five thermal cycles, which aim to compare the influence of different electric measurement conditions (electric stress). Compared with the second and the third thermal cycles, the first thermal cycle represents more

measurements, including not only transfer, but also rather time-consuming output characteristics in every measurement point. The 4^{th}-6^{th} thermal cycles were conducted using the same gate voltage and drain-source voltage, but with different temperature intervals or different temperature ranges. The *I-T* curves extracted from these experiments are shown in Figure S5. Nearly all the curves show a positive slope during the thermal cycles, which is consistent with an ordinary thermal activation process of the conduction. However, we can observe a systematic decrease of the current intensity during the first five heating ramps above ca. 70-75 °C, which indicates that the device underwent degradation in these conditions. Most importantly, it turns out that the degradation occurs as a combined effect of high temperature and applied voltage. Then, by decreasing the effective measurement time (Cycles 2 & 3) it is possible to reach a reasonably good reversibility with a current drop $(I_{final}-I_{initial})/I_{initial}$ of ca. -10-20 %. What is more, cycles 2 and 3 were obtained from transfer characteristics, which contain potentially more information as simple *I-T* curves measured at fixed gate and drain-source voltages. Overall, these tests confirmed that, unfortunately, the devices are rather sensitive to combined voltage/temperature stress, but with some care, temperature-dependent transfer characteristics can be acquired with an acceptable reproducibility.

Table S1: Parameters of six successive temperature cycles of a standard device.

Thermal cycles	Measurements
1^{st} (45-85-45 °C)	**Output and Transfer (V_{DS} = -2,-5,-10 & -50 V) characteristics, temperature interval = 5 °C**
2^{nd} (45-85-45 °C)	**Transfer (V_{DS}= -2 & -5 V) characteristics, temperature interval = 10 °C**
3^{rd} (45-85-45 °C)	**Transfer (V_{DS}= -10 & -50 V) characteristics, temperature interval = 10 °C**
4^{th} (45-85-45 °C)	**I-T characteristic (V_G = -30 V, V_{DS} = -10 V), temperature interval = 0.083 °C, 5 °C/min**
5^{th} (45-85-45 °C)	**I-T characteristic (V_G = -30 V, V_{DS} = -10 V), temperature interval = 1 °C, 5 °C/min**
6^{th} (45-65-45 °C)	**I-T characteristic (V_G = -30 V, V_{DS} = -10 V), temperature interval = 1 °C, 5 °C/min**

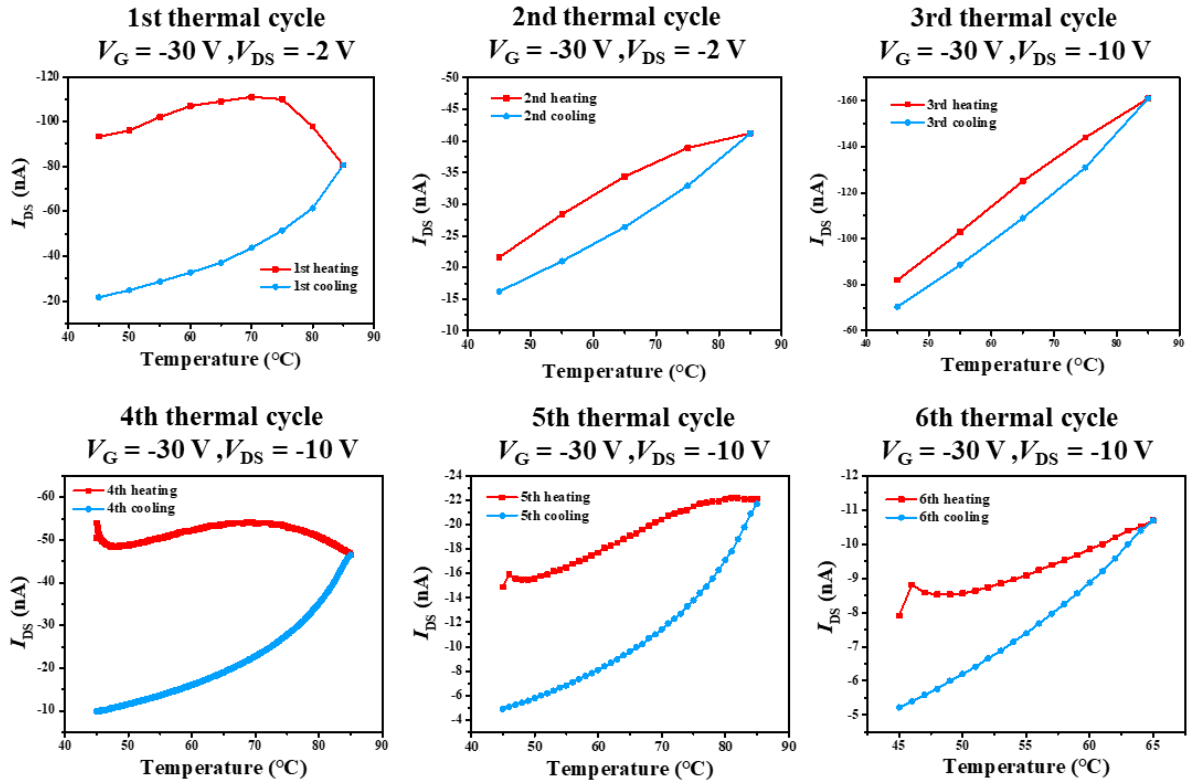

Figure S5: Current-temperature (*I-T*) characteristics of a standard device for six successive thermal cycles under different measurement conditions – shown in Table S1. (The data for the first three thermal cycles were extracted from the transfer characteristics.)